

DTIC FILE COPY

4

OFFICE OF NAVAL RESEARCH

Contract N00014-86-K-0043

TECHNICAL REPORT No. 97

Nonresonant Interaction of a Three-Level Atom with Cavity Fields  
IV. Atomic Dipole Moment and Squeezing Effects

by

Xiao-shen Li, D. L. Lin, Thomas F. George and Xhen-dong Liu

Prepared for Publication

in

Physical Review A

Departments of Chemistry and Physics  
State University of New York at Buffalo  
Buffalo, New York 14260

April 1989

Reproduction in whole or in part is permitted for any purpose of the  
United States Government.

This document has been approved for public release and sale;  
its distribution is unlimited.

DTIC  
ELECTE  
APR 18 1989  
S H D  
JF

89 4 18 053

AD-A206 788

UNCLASSIFIED

SECURITY CLASSIFICATION OF THIS PAGE

## REPORT DOCUMENTATION PAGE

Form Approved  
OMB No. 0704-0188

1a. REPORT SECURITY CLASSIFICATION <b>Unclassified</b>			1b. RESTRICTIVE MARKINGS		
2a. SECURITY CLASSIFICATION AUTHORITY			3. DISTRIBUTION / AVAILABILITY OF REPORT Approved for public release; distribution unlimited		
2b. DECLASSIFICATION / DOWNGRADING SCHEDULE					
4. PERFORMING ORGANIZATION REPORT NUMBER(S)  UBUFFALO/DC/89/TR-97			5. MONITORING ORGANIZATION REPORT NUMBER(S)		
6a. NAME OF PERFORMING ORGANIZATION Depts. Chemistry & Physics State University of New York		6b. OFFICE SYMBOL (If applicable)	7a. NAME OF MONITORING ORGANIZATION		
6c. ADDRESS (City, State, and ZIP Code) Fronczak Hall, Amherst Campus Buffalo, New York 14260			7b. ADDRESS (City, State, and ZIP Code) Chemistry Program 800 N. Quincy Street Arlington, Virginia 22217		
8a. NAME OF FUNDING / SPONSORING ORGANIZATION Office of Naval Research		8b. OFFICE SYMBOL (If applicable)	9. PROCUREMENT INSTRUMENT IDENTIFICATION NUMBER  Contract N00014-86-K-0043		
8c. ADDRESS (City, State, and ZIP Code) Chemistry Program 800 N. Quincy Street Arlington, Virginia 22217			10. SOURCE OF FUNDING NUMBERS		
			PROGRAM ELEMENT NO.	PROJECT NO.	TASK NO.
					WORK UNIT ACCESSION NO.
11. TITLE (Include Security Classification) Nonresonant Interaction of a Three-Level Atom with Cavity Fields IV. ATOMIC Dipole Moment and Squeezing Effects					
12. PERSONAL AUTHOR(S) Xiao-shen Li, D. L. Lin, <u>Thomas F. George</u> and Zhen-dong Liu					
13a. TYPE OF REPORT		13b. TIME COVERED FROM _____ TO _____		14. DATE OF REPORT (Year, Month, Day) April 1989	
				15. PAGE COUNT 37	
16. SUPPLEMENTARY NOTATION Prepared for publication in Physical Review A					
17. COSATI CODES			18. SUBJECT TERMS (Continue on reverse if necessary and identify by block number)		
FIELD	GROUP	SUB-GROUP	THREE-LEVEL ATOM, ATOMIC DIPOLE MOMENT		
			CAVITY FIELDS, CORRELATION FUNCTION		
			NONRESONANT INTERACTION, SQUEEZING EFFECTS		
19. ABSTRACT (Continue on reverse if necessary and identify by block number)					
<p>The behavior of the dipole moment of a three-level atom interacting with cavity fields of arbitrary detunings is investigated. The time evolution and squeezing conditions of the components and correlation function of the dipole moment are calculated for three cases: one-mode field and a <math>\Sigma</math>-type atom initially in the upper state, two-mode field and a <math>\Lambda</math>-type atom initially in the upper state, and two-mode field and a <math>\Lambda</math>-type atom initially in one of the lower states. A number of interesting features are found and discussed.</p>					
20. DISTRIBUTION / AVAILABILITY OF ABSTRACT <input checked="" type="checkbox"/> UNCLASSIFIED/UNLIMITED <input checked="" type="checkbox"/> SAME AS RPT. <input type="checkbox"/> DTIC USERS			21. ABSTRACT SECURITY CLASSIFICATION Unclassified		
22a. NAME OF RESPONSIBLE INDIVIDUAL Dr. David L. Nelson			22b. TELEPHONE (Include Area Code) (202) 696-4410		22c. OFFICE SYMBOL

Physical Review A, in press

Nonresonant interaction of a three-level atom with cavity fields

IV. Atomic dipole moment and squeezing effects

Xiao-shen Li

Center of Theoretical Physics

Chinese Center of Advanced Science and Technology (World Laboratory)

P.O. Box 8730, Beijing 100080, People's Republic of China

and

Shanghai Institute of Metallurgy, Chinese Academy of Sciences

Shanghai, People's Republic of China

D.L. Lin and Thomas F. George

Department of Physics and Astronomy

State University of New York at Buffalo

Amherst, New York 14260

Zhen-dong Liu

Center of Theoretical Physics

Chinese Center of Advanced Science and Technology (World Laboratory)

P.O. Box 8730, Beijing 100080, People's Republic of China

and

Department of Physics, Jiangxi Normal University

Nanchang, Jiangxi, People's Republic of China

### Abstract

The behavior of the dipole moment of a three-level atom interacting with cavity fields of arbitrary detunings is investigated. The time evolution and squeezing conditions of the components and correlation function of the dipole moment are calculated for three cases: one-mode field and a  $\Xi$ -type atom initially in the upper state, two-mode field and a  $\Lambda$ -type atom initially in the upper state, and two-mode field and a  $\Lambda$ -type atom initially in one of the lower states. A number of interesting features are found and discussed.

1987 PACS numbers: 32.80-t 42.50-p 42.50.Dv

## I. Introduction

It is now well known that an atomic system driven by one or two modes of a cavity field exhibits many remarkable phenomena such as the collapse and revival of Rabi oscillations<sup>1-5</sup>, antibunching<sup>6</sup>, squeezing<sup>7-14</sup> and so forth. The collapse and revival phenomenon has recently been observed for the first time with Rydberg atoms in a superconducting cavity<sup>15</sup>. The interaction between light and matter can also bring about a kind of purely quantum mechanical set of states known as squeezed states, which have attracted a great deal of interest in recent years<sup>16-30</sup>. A number of nonlinear optical systems can generate squeezed states. Theoretical interest has been mainly in minimum uncertainties of the squeezed light<sup>16-20</sup>, and the first experimental observation of such squeezed states has been realized<sup>21</sup> with four-wave mixing in sodium atoms. A subsequent experiment<sup>22</sup> has reported the observation of stronger squeezing in the down-conversion parametric process. Since the squeezed light has greatly enhanced signal-to-noise ratios, it has high potential of applications in optical communication<sup>27</sup>, detection of gravitational waves<sup>20,28</sup>, laser spectroscopy<sup>29</sup> and many other possibilities.

We are more interested in the squeezing phenomenon in the interaction of an atom with the cavity field. The field squeezing in a two-level Jaynes-Cummings (J-C) model<sup>7</sup> was found to be about 19% at most. In the case of a three-level  $\Xi$ -type atom interacting with one-mode cavity field, the maximum squeezing was found to be about<sup>11</sup> 31%. For a four-level cascade atom in the one-mode J-C model, 36% maximum squeezing has been predicted<sup>12</sup>.



For	<input checked="checked" type="checkbox"/>
&I	<input type="checkbox"/>
ed	<input type="checkbox"/>
ton	
ton/	
lity Codes	
and/or	
cial	

A-1

As a matter of fact, when multiphoton processes are considered<sup>10</sup>, the maximum squeezing can be as high as 57%.

We investigate, in this paper, the time evolution as well as the squeezing in the interaction between a three-level atom and one- or two-mode cavity fields. The evolution of an atomic dipole moment in a two-level J-C model has been studied by different authors<sup>31-33</sup>. They have discovered that the quantum mechanical nature of the interaction is reflected through the behavior of the atomic dipole moment. Thus we expect that atomic dipole moments should have squeezing.

The squeezing of an operator is in general defined in the following manner. When two arbitrary operators A and B of the same physical dimension obey the commutation relation  $[A, B] = C$ , they satisfy the uncertainty relation  $\Delta A \Delta B \geq \frac{1}{2} |\langle C \rangle|$ . Squeezing occurs whenever one of the observables satisfies the relation

$$(\Delta A)^2 < \frac{1}{2} |\langle C \rangle| \quad (1a)$$

$$(\Delta B)^2 < \frac{1}{2} |\langle C \rangle|. \quad (1b)$$

The plan of this paper is as follows. We first review briefly in Sec. II the theory of a generalized J-C model in which a three-level atom interacts with cavity fields of arbitrary detunings. The mean values of the component and correlation operators of the atomic dipole moment are calculated in Sec. III along with the squeezing conditions. Results of our numerical computation are presented and discussed in Sec. IV, and finally we make a few concluding remarks in Sec. V.

## II. Theory

The general formalism of a three-level atom interacting with cavity fields is given in detail in Ref. 4 (hereafter referred to as I). Here we merely outline what is essential for our present discussion of the evolution and squeezing of the atomic dipole moment. We consider two atomic level configurations, namely the  $\Xi$ -type and  $\Lambda$ -type as shown in Fig. 1. For the initial states, the atom may start in either  $|a\rangle$  or  $|b\rangle$  while the field is assumed to be in the coherent state.

The Hamiltonian is, in the interaction picture,

$$H = \hbar(H_0 + H_1) \quad (2)$$

where, for the one-mode  $\Xi$ -type case,

$$H_0 = \sum_{\eta=a,b,c} \omega_{\eta} A_{\eta}^{\dagger} A_{\eta} + \Omega a^{\dagger} a \quad (3)$$

$$H_1 = \lambda_1 e^{i\Delta_1 t} a A_b^{\dagger} A_a + \lambda_2 e^{i\Delta_2 t} a A_a^{\dagger} A_c + \text{h.c.} \quad (4)$$

$$\Delta_1 = -(\Omega - \omega_b + \omega_a), \quad \Delta_2 = \Omega - \omega_a + \omega_c,$$

and for the two mode  $\Lambda$ -type case,

$$H_0 = \sum_{\eta=a,b,c} \omega_{\eta} A_{\eta}^{\dagger} A_{\eta} + \sum_{i=1,2} \Omega_i a_i^{\dagger} a_i \quad (5)$$

$$H_1 = \lambda_1 e^{i\Delta_1 t} a_1 A_a^{\dagger} A_b + \lambda_2 e^{i\Delta_2 t} a_2 A_a^{\dagger} A_c + \text{h.c.} \quad (6)$$

$$\Delta_1 = \Omega_1 - \omega_a + \omega_b, \quad \Delta_2 = \Omega_2 - \omega_a + \omega_c.$$

The operators in the Hamiltonian are defined as follows:  $A_{\eta}^{\dagger}$  creates an atom

in the state  $|\eta\rangle$ ,  $a^{\dagger}$  creates a photon,  $\lambda_i$  are the usual coupling constants and  $\Delta_i$  are the detuning parameters.

As has been shown in I, the Schrödinger equation can be solved by the state vector

$$|\psi(t)\rangle = \sum_n Q(n) [A(n+1, t) |a, n+1\rangle + B(n, t) |b, n\rangle + C(n+2, t) |c, n+2\rangle] \quad (7a)$$

for the one-mode E-type case with the atom initially in  $|b\rangle$ , or

$$|\psi(t)\rangle = \sum_{n_1, n_2} Q_1(n_1) Q_2(n_2) [A(n_1-1, n_2, t) |a, n_1-1, n_2\rangle + B(n_1, n_2, t) |b, n_1, n_2\rangle + C(n_1-1, n_2+1, t) |c, n_1-1, n_2+1\rangle] \quad (7b)$$

for the two-mode A-type with the atom initially in  $|b\rangle$ , or

$$|\psi(t)\rangle = \sum_{n_1, n_2} Q_1(n_1) Q_2(n_2) [A(n_1, n_2, t) |a, n_1, n_2\rangle + B(n_1+1, n_2, t) |b, n_1+1, n_2\rangle + C(n_1, n_2+1, t) |c, n_1, n_2+1\rangle] \quad (7c)$$

for the two-mode A-type case with the atom initially in  $|a\rangle$ . The corresponding initial conditions are for the one-mode case,

$$|\psi(0)\rangle = |\eta, \xi\rangle = |\eta\rangle \sum_n Q(n) |n\rangle, \quad (8a)$$

and for the two-mode case,

$$|\psi(0)\rangle = |\eta, \xi_1, \xi_2\rangle = |\eta\rangle \sum_{n_1, n_2} Q_1(n_1) Q_2(n_2) |n_1, n_2\rangle. \quad (8b)$$

where  $n$  is the photon number and  $n_i$  is the photon number referring to the mode  $i$ . The probability amplitudes in (7) are

$$A = -e^{i\Delta_2 t} \sum_{i=1}^3 U_i \mu_i e^{i\mu_i t} \quad (9a)$$

$$B = \frac{1}{V_1} e^{i(\Delta_1 - \Delta_2)t} \sum_{i=1}^3 U_i (\mu_i^2 - \Delta_2 \mu_i - V_2^2) e^{i\mu_i t} \quad (9b)$$

$$C = V_2 \sum_{i=1}^3 U_i e^{i\mu_i t}, \quad (9c)$$

where

$$\mu_1 = -\frac{1}{3} x_1 + \frac{2}{3} (x_1^2 - 3x_2)^{1/2} \cos \theta \quad (10a)$$

$$\mu_2 = -\frac{1}{3} x_1 + \frac{2}{3} (x_1^2 - 3x_2)^{1/2} \cos(\theta + \frac{2}{3}\pi) \quad (10b)$$

$$\mu_3 = -\frac{1}{3} x_1 + \frac{2}{3} (x_1^2 - 3x_2)^{1/2} \cos(\theta + \frac{4}{3} \pi) \quad (10c)$$

$$\theta = \frac{1}{3} \cos^{-1} \left[ \frac{9x_1x_2 - 2x_1^3 - 27x_3}{2(x_1^2 - 3x_2)^{3/2}} \right] \quad (10d)$$

and

$$x_1 = \Delta_1 - 2\Delta_2 \quad (11a)$$

$$x_2 = -[V_1^2 + V_2^2 + \Delta_2(\Delta_1 - \Delta_2)] \quad (11b)$$

$$x_3 = (\Delta_2 - \Delta_1) V_2^2 \quad (11c)$$

The probability amplitudes for the one- and two-mode cases take the same expressions as (9) and depend on the photon number in different modes through the coupling strength parameters  $V_1$  and  $V_2$ . The explicit forms of these parameters are listed in Table 1 of I for various cases.

The atomic level occupation probabilities can be found directly from (7) and (9). They are

$$P_a(t) = \sum_n p(n) |A(n+1, t)|^2 \quad (12a)$$

$$P_b(t) = \sum_n p(n) |B(n, t)|^2 \quad (12b)$$

$$P_c(t) = \sum_n p(n) |C(n, t)|^2 \quad (12c)$$

for the one-mode  $\Xi$ -type case with initial atomic state  $|b\rangle$ ,

$$P_a(t) = \sum_{n_1 n_2} p(n_1, n_2) |A(n_1-1, n_2, t)|^2 \quad (13a)$$

$$P_b(t) = \sum_{n_1 n_2} p(n_1, n_2) |B(n_1, n_2, t)|^2 \quad (13b)$$

$$P_c(t) = \sum_{n_1 n_2} p(n_1, n_2) |C(n_1-1, n_2+1, t)|^2 \quad (13c)$$

for the two-mode  $\Lambda$ -type case with initial atomic state  $|b\rangle$ , and

$$P_a(\tau) = \sum_{n_1 n_2} p(n_1, n_2) |A(n_1, n_2, \tau)|^2 \quad (14a)$$

$$P_b(\tau) = \sum_{n_1 n_2} p(n_1, n_2) |B(n_1 + 1, n_2, \tau)|^2 \quad (14b)$$

$$P_c(\tau) = \sum_{n_1 n_2} p(n_1, n_2) |C(n_1, n_2 + 1, \tau)|^2 \quad (14c)$$

for the two-mode  $\Lambda$ -type case with initial atomic state  $|a\rangle$ , where

$P(n) = |Q(n)|^2$  and  $p(n_1, n_2) = |Q_1(n_1)|^2 |Q_2(n_2)|^2$  are the initial photon distributions for the one and two-mode cases, respectively. In the present work, we assume the field to be in the coherent state initially. Therefore

$$Q(n) = \frac{\alpha^n}{\sqrt{n!}} e^{-\bar{n}/2} \quad (15a)$$

$$P(n) = \bar{n}^n e^{-\bar{n}} / n! \quad (15b)$$

$$Q_i(n_i) = \frac{\alpha_i^{n_i}}{\sqrt{n_i!}} e^{-\bar{n}_i/2}, \quad i=1,2 \quad (15c)$$

$$P(n_1, n_2) = \bar{n}_1^{n_1} \bar{n}_2^{n_2} e^{-(\bar{n}_1 + \bar{n}_2)} / n_1! n_2! \quad (15d)$$

where  $|\alpha|^2 = \bar{n}$  and  $|\alpha_i|^2 = \bar{n}_i$ .

### III. The atomic dipole moment and squeezing effects

To investigate the time evolution as well as the squeezing of the atomic dipole moment, we restrict our discussions to the envelope of the mean value of dipole moment component and correlation operators. Thus it is understood from now on that, similar to Refs. 31-33, we actually refer to their envelopes when we calculate the component operators

$$S_{ab} = |A\rangle\langle b| e^{-i\omega_{ab}\tau} = S_{ba}^\dagger \quad (16a)$$

$$S_{ac} = |A\rangle\langle c| e^{-i\omega_{ac}t} = S_{ca}^\dagger \quad (16b)$$

and the correlation operator

$$S_{bc} = S_{ba} S_{ac} = |b\rangle\langle c| e^{-i\omega_{bc}t} = S_{cb}^\dagger. \quad (16c)$$

The dispersive parts of these operators are defined as

$$d_{ab}^I = \frac{1}{2} (S_{ab} + S_{ba}) \quad (17a)$$

$$d_{ac}^I = \frac{1}{2} (S_{ac} + S_{ca}) \quad (17b)$$

$$d_{bc}^I = \frac{1}{2} (S_{bc} + S_{cb}), \quad (17c)$$

and the absorptive parts are

$$d_{ab}^{II} = \frac{1}{2i} (S_{ab} - S_{ba}) \quad (18a)$$

$$d_{ac}^{II} = \frac{1}{2i} (S_{ac} - S_{ca}) \quad (18b)$$

$$d_{bc}^{II} = \frac{1}{2i} (S_{bc} - S_{cb}) \quad (18c)$$

These operators satisfy the commutation relations

$$[d_{ab}^I, d_{ab}^{II}] = \frac{1}{2i} (S_{bb} - S_{aa}) \quad (19a)$$

$$[d_{ac}^I, d_{ac}^{II}] = \frac{1}{2i} (S_{cc} - S_{aa}) \quad (19b)$$

$$[d_{bc}^I, d_{bc}^{II}] = \frac{1}{2i} (S_{cc} - S_{bb}), \quad (19c)$$

where  $S_{aa} = |a\rangle\langle a|$ ,  $S_{bb} = |b\rangle\langle b|$  and  $S_{cc} = |c\rangle\langle c|$  are the occupation

operators for the three atomic levels, respectively. Hence, according to

(1), squeezing occurs whenever any of the following conditions are

satisfied,

$$(\Delta d_{ab}^I)^2 < \frac{1}{4} | \langle S_{bb} - S_{aa} \rangle | \quad (20a)$$

$$(\Delta d_{ac}^{\xi})^2 < \frac{1}{4} |\langle S_{cc} - S_{aa} \rangle| \quad (20b)$$

$$(\Delta d_{bc}^{\xi})^2 < \frac{1}{4} |\langle S_{cc} - S_{bb} \rangle|, \quad (20c)$$

where the symbol  $\xi$  stands for the superscript I or II.

To simplify the expressions, we introduce the notation

$$D_{ab}^{\xi} = (\Delta d_{ab}^{\xi})^2 / |P_b - P_a| \quad (21a)$$

$$D_{ac}^{\xi} = (\Delta d_{ac}^{\xi})^2 / |P_c - P_a| \quad (21b)$$

$$D_{bc}^{\xi} = (\Delta d_{bc}^{\xi})^2 / |P_b - P_c| \quad (21c)$$

By noting the atomic level occupation probabilities  $P_{\eta} = \langle S_{\eta\eta} \rangle$ ,

( $\eta = a, b, c$ ), the conditions (20) then reduce to

$$D_{ab}^{\xi}, D_{ac}^{\xi}, D_{bc}^{\xi} < \frac{1}{4} \quad (22)$$

It is now not difficult to find from the above relations that

$$D_{ab}^I = [\frac{1}{4} (1 - P_c) - (\text{Re} \langle S_{ab} \rangle)^2] / |P_a - P_b| \quad (23a)$$

$$D_{ab}^{II} = [\frac{1}{4} (1 - P_c) - (\text{Im} \langle S_{ab} \rangle)^2] / |P_a - P_b| \quad (23b)$$

$$D_{ac}^I = [\frac{1}{4} (1 - P_b) - (\text{Re} \langle S_{ac} \rangle)^2] / |P_a - P_c| \quad (23c)$$

$$D_{ac}^{II} = [\frac{1}{4} (1 - P_b) - (\text{Im} \langle S_{ac} \rangle)^2] / |P_a - P_c| \quad (23d)$$

$$D_{bc}^I = [\frac{1}{4} (1 - P_a) - (\text{Re} \langle S_{bc} \rangle)^2] / |P_b - P_c| \quad (23e)$$

$$D_{bc}^{II} = [\frac{1}{4} (1 - P_a) - (\text{Im} \langle S_{bc} \rangle)^2] / |P_b - P_c| \quad (23f)$$

#### IV. Results and Discussions

We study the component and correlation operators of the atomic dipole moment for three different cases: the one-mode  $\Xi$ -type with the atom in  $|b\rangle$

initially, the two-mode  $\Lambda$ -type with the atom in  $|a\rangle$  initially and the two-mode  $\Lambda$ -type with initial atomic state  $|b\rangle$ . The initial photon state is assumed to be the coherent state (15) for all the cases. The mean values of these operators are given by

$$\langle S_{ab} \rangle = \text{Tr}(|\psi(t)\rangle\langle\psi(t)|a\rangle\langle b|) \quad (24a)$$

$$\langle S_{ac} \rangle = \text{Tr}(|\psi(t)\rangle\langle\psi(t)|a\rangle\langle c|) \quad (24b)$$

$$\langle S_{bc} \rangle = \text{Tr}(|\psi(t)\rangle\langle\psi(t)|b\rangle\langle c|), \quad (24c)$$

where we have made use of the density matrix  $\rho(t) = |\psi(t)\rangle\langle\psi(t)|$ . Explicit calculations are made separately for each of these cases in the following. Throughout the numerical work, we have assumed the same coupling constants  $\lambda_1 = \lambda_2 = \lambda$  for the two modes, and employed the units  $\lambda$  and  $1/\lambda$  for energy and time, respectively.

#### A. One-mode $\Xi$ -type with initial atomic state $|b\rangle$

We first look up from Table 1 of I for this particular case the coefficients found in Eq. (9),

$$U_1 = V_1/\mu_{12}\mu_{13} \quad (25a)$$

$$U_2 = V_2/\mu_{21}\mu_{23} \quad (25b)$$

$$U_3 = V/\mu_{31}\mu_{32} \quad (25c)$$

where  $V_1^2 = \lambda_1^2 (n+1)$ ,  $V_2^2 = \lambda_2^2 (n+2)$ , and  $\mu_{ij} = \mu_i - \mu_j$ . Substituting (25) in (7a) and making use of (8)-(11), we find

$$\begin{aligned} \langle S_{ab} \rangle &= \sum_n Q(n) Q^*(n-1) A^*(n) B(n) \\ &= \bar{n}^{-1/2} \sum_n \sqrt{n} p(n) A^*(n) B(n) \end{aligned} \quad (26a)$$

$$\langle S_{ac} \rangle = \bar{n}^{-3/2} \sum_n \sqrt{n-1} n p(n) A^*(n) C(n) \quad (26b)$$

$$\langle S_{bc} \rangle = \bar{n}^{-1} \sum_n \sqrt{n(n-1)} p(n) B^*(n) C(n), \quad (26c)$$

where we have assumed the initial photon distribution to be coherent as given by (15). The time dependence of the probability amplitudes A, B and C is understood although it is not explicitly marked.

The real and imaginary parts of the quantities in (26) are numerically computed and plotted as functions of time in Figs. 2 and 3 for different choices of detuning parameters. It is observed from these figures that the time dependence appears like Rabi oscillation with oscillatory changing amplitudes. Compared to the collapse and revival of the atomic level occupation probabilities presented in I, we find that  $\langle S_{ab} \rangle$ ,  $\langle S_{ac} \rangle$ , and  $\langle S_{bc} \rangle$  are still oscillating during the time when the occupation probabilities are collapsed. This indicates that the relative phase between the pair of states between which the atom makes transitions keeps changing, and at the same time the atomic transitions are in dynamical equilibrium.

In general,  $\langle S_{ab} \rangle$ ,  $\langle S_{ac} \rangle$  and  $\langle S_{bc} \rangle$  are superpositions of oscillations with high and low frequencies, and the phenomenon of quantum collapse and revival appears mainly in the high frequency component. This is clearly depicted in Fig. 3 especially for  $\langle S_{bc} \rangle$ . A similar situation occurs also for different detuning parameters at two-photon resonance. Furthermore, we see from Fig. 3 that the amplitudes of  $\langle S_{ab} \rangle$  and  $\langle S_{ac} \rangle$  are very small compared to that of  $\langle S_{bc} \rangle$  which is associated with two-photon processes.

This may be called quasi-coherent trapping phenomenon<sup>3</sup> and is easily understandable if we note that the detunings are far from one-photon resonances even though they satisfy two-photon resonance.

We now turn our attention to squeezing phenomena by computing the quantities in (23). It is interesting to find that any of these six components can be made to show squeezing by suitably choosing the parameters  $\bar{n}$ ,  $\Delta_1$  and  $\Delta_2$ . We also discover after analyzing our results that the squeezing of  $D_{ab}^{II}$  is more remarkable than the others. Some of the results calculated from (23b) are presented in Figs. 4 and 5 in which a horizontal line at  $1/4$  is drawn as a reference. Whenever the curve crosses below this line the quantity is squeezed.  $D_{ab}^I$  calculated for the same conditions are also shown in Fig. 4 for comparison. In all the cases, we observe that the atom enters the squeezed state right after the interaction takes place, and the squeezing increases with time until it reaches the maximum depth. With weak excitation, the atom is found in the squeezed state only once. This is completely different from the field squeezing in the J-C model<sup>7-13</sup>. It is also clear from these curves that the maximum squeezing depth of  $D_{ab}^{II}$  depends mainly upon the atomic transition  $|b\rangle \leftrightarrow |a\rangle$ . When the field is at resonance with this transition, its squeezing deepens. When  $\Delta_1$  and  $\Delta_2$  have opposite signs and are far away from resonance conditions, the squeezing weakens. Our numerical study shows no indication of strong influence of the two-photon resonance.

We also plot in Fig. 5 the maximum squeezing depth as well as the time at which the maximum squeezing appears as a function of the initial excitation intensity  $\bar{n}$ . The maximum squeezing increases with  $\bar{n}$  and gradually saturates. At the same time, it shows that for larger  $\bar{n}$  the maximum squeezing occurs earlier. When  $\bar{n} \geq 1000$ ,  $D_{ab}^{II} \sim 0.1$  and the maximum

squeezing -60%. This is a larger squeezing than reported in the literature<sup>7-13</sup>.

B. Two-mode  $\Lambda$ -type with the atom initially in  $|a\rangle$

The coefficients for this case are found from Table 1 of I to be

$$U_1 = - \frac{\mu_1 + \Delta_{12}}{\mu_{12}\mu_{13}} \quad (27a)$$

$$U_2 = - \frac{\mu_2 + \Delta_{12}}{\mu_{21}\mu_{23}} \quad (27b)$$

$$U_3 = - \frac{\mu_3 + \Delta_{12}}{\mu_{31}\mu_{32}} \quad (27c)$$

where

$$V_1^2 = \lambda_1^2 (n_1 + 1), \quad V_2^2 = \lambda_2^2 (n_2 + 1). \quad \text{Following the same procedures}$$

outlined above, we find

$$\langle S_{ab} \rangle = \bar{n}^{-1/2} \sum_{n_1, n_2} \sqrt{n_1} A^*(n_1, n_2) B(n_1, n_2) p(n_1, n_2) \quad (28a)$$

$$\langle S_{ac} \rangle = \bar{n}^{-1/2} \sum_{n_1, n_2} \sqrt{n_2} A^*(n_1, n_2) C(n_1, n_2) p(n_1, n_2) \quad (28b)$$

$$\langle S_{bc} \rangle = (\bar{n}_1 \bar{n}_2)^{-1/2} \sum_{n_1, n_2} \sqrt{n_1 n_2} B^*(n_1, n_2) C(n_1, n_2) p(n_1, n_2). \quad (28c)$$

Again, the real and imaginary parts of (28) are separately computed and plotted in Figs. 6 and 7. Rabi oscillations still show quantum collapse and revival phenomena, but the behavior is quite different from the one-mode case.  $S_{bc}$  vibrates with almost zero amplitude, whether or not the two-photon resonance condition is satisfied. This implies that two-photon processes are negligible in this case, in agreement with the conclusions of

Ref. 2. Furthermore, we find no sign of squeezing in our numerical study for this case.

### C. Two-mode A-type with initial atomic state $|b\rangle$

The U's for this case are the same as 25) according to Table 1 of I, but the V's are given by  $V_1^2 = \lambda_1^2 n_1$  and  $V_2^2 = \lambda_2^2 (n_2 + 1)$ . The equations for the operator mean values can be obtained in the same fashion as (26). Thus

$$\langle S_{ab} \rangle = \bar{n}_1^{-\frac{1}{2}} \sum_{n_1, n_2} (n_1 + 1)^{-\frac{1}{2}} A^*(n_1, n_2) B(n_1, n_2) p(n_1, n_2) \quad (29a)$$

$$\langle S_{ac} \rangle = \bar{n}_1 \bar{n}_2^{-\frac{1}{2}} \sum_{n_1, n_2} \sqrt{n_2} (n_1 + 1)^{-1} A^*(n_1, n_2) C(n_1, n_2) p(n_1, n_2) \quad (29b)$$

$$\langle S_{bc} \rangle = \sqrt{\bar{n}_1 / \bar{n}_2} \sum_{n_1, n_2} \left( \frac{n_2}{n_1 + 1} \right)^{\frac{1}{2}} B^*(n_1, n_2) C(n_1, n_2) p(n_1, n_2). \quad (29c)$$

Numerical results for these equations are presented in Figs. 8-10. Here we discover that  $\langle S_{ab} \rangle$  is a typical example for the superposition of high- and low-frequency oscillations. This becomes particularly clear when the field resonance is at resonance with the transition  $|b\rangle \rightarrow |a\rangle$ , as can be seen in Fig. 9. As a matter of fact, similar phenomena exist in the above case as is shown in Fig. 6. For given  $\bar{n}_1$  and  $\bar{n}_2$ , the oscillation frequency of  $\langle S_{ab} \rangle$  is largely determined by  $\Delta_1$ . In fact, it is found to increase with increasing  $|\Delta_1|$ . In addition, we also note that the large amplitude in Fig. 10(f) reflects the dominant effect of two-photon process as in the case of Fig. 3.

In our study of the squeezing in this case, we discover that the atom can be put in the squeezed state at certain time by suitably choosing the

parameters  $\bar{n}_1$ ,  $\bar{n}_2$ ,  $\Delta_1$  and  $\Delta_2$ . Taking again  $D_{ab}^{I,II}$  as examples, we plot part of the results in Fig. 11, which appear quite different from the one-mode case. As time increases, the atom can oscillate between squeezed and non-squeezed states when the excitation is not strong. From Figs. 11(a)-(c), we see how the squeezing depth changes by varying detunings. A comparison of 11(b) and 11(f) indicates that  $\Delta_2 = 0$  is more favorable for squeezing. Hence stronger squeezing may be expected by strengthening the coupling between the two transitions. On the other hand, the choice of the excitation intensity  $\bar{n}_1$  is of great importance as can be seen by comparing (b), (d), (e), (g) and (h) in Fig. 11.

From the above analyses we note that the squeezing in the two-mode case is in general not as strong as in the one-mode case. When  $\Delta_1$  is sufficiently large the atom is found to jump between squeezed and coherent states for quite some time. Fig. 11(c) illustrates such a typical case. As a final remark, we note that the two curves may intersect or even coincide with the horizontal line at the same time as in Fig. 11(c), (d), (g) and (h). When this is the case, the condition of minimum uncertainties is satisfied, namely

$$\Delta d_{ab}^I \Delta d_{ab}^{II} = 1/4 | \langle S_{bb} - S_{aa} \rangle |. \quad (30)$$

## V. Conclusion

On the basis of a numerical study, we have analyzed the evolution and squeezing of the dipole moment of a three-level atom interacting with one- or two-mode cavity fields with arbitrary detunings. Only part of the large amount is presented here. The Rabi oscillations show collapse and revival

with qualitatively different behavior from those of the atomic level occupation probabilities. For the three cases we have considered, the two-mode  $\Lambda$ -type case with initial atomic state in  $|a\rangle$  does not show any squeezing effect. For the other two cases, we have found that the dipole moment squeezing depends upon one-photon processes while the correlation function squeezing is related to two-photon processes. When the one-mode field couples with two atomic transitions, stronger coupling leads to deeper squeezing. A maximum squeezing of about 60% can be reached according to our calculation.

As we know, there exists a simple relation between the squeezing of the dipole moment and the field squeezing in the case of resonance fluorescence<sup>24</sup>. In the present case, however, we can not find such a simple relation between the field squeezing and the atomic squeezing. The quantized electric field in a lossless cavity is no longer related to the dipole lowering operator in a simple manner. We try to analyze the situation in what follows by considering the one-mode  $\Xi$ -type atom. The total dipole moment operator of the atom is

$$D = S_{ba} + S_{ac}. \quad (31)$$

The dispersive and absorptive parts are

$$d^I = \frac{1}{2} (D + D^\dagger) \quad (32a)$$

$$d^{II} = \frac{1}{2} (D - D^\dagger) \quad (32b)$$

respectively, and their corresponding variances are

$$(\Delta d^I)^2 = \frac{1}{4} (1 + P_a + 2\text{Re}\langle S_{ba} \rangle) - (\text{Re}\langle S_{ab} \rangle + \text{Re}\langle S_{ac} \rangle)^2, \quad (33a)$$

$$(\Delta d^{II})^2 = \frac{1}{4} (1 + P_a - 2\text{Re}\langle S_{ba} \rangle) - (\text{Im}\langle S_{ab} \rangle + \text{Im}\langle S_{ac} \rangle)^2. \quad (33b)$$

Similar to (21) and (22), it can be shown that the condition for squeezing is

$$D^{\xi} = \frac{(\Delta d^{\xi})^2}{|P_b - P_c|} < \frac{1}{4}. \quad (34)$$

The variances of one-mode cavity field quadratures are

$$(\Delta d_1)^2 = \frac{1}{4} [1 + 2\langle n \rangle + 2\text{Re}\langle a^2 \rangle - 4(\text{Re}\langle a \rangle)^2], \quad (35a)$$

$$(\Delta d_2)^2 = \frac{1}{4} [1 + 2\langle n \rangle + 2\text{Re}\langle a^2 \rangle - 4(\text{Im}\langle a \rangle)^2]. \quad (35b)$$

For easier comparison, we plot in Fig. 12, the squeezing of the dipole moment as a function of time, and the variances of the field fluctuation are plotted in Fig. 13. Evidently, the squeezing of these quantities do not occur at the same time. The two parts of the atomic dipole moment show squeezing alternatively, while in the case of field only  $d_1$  shows squeezing. When the two-photon resonance condition is satisfied, it is observed from Fig. 13(b) that the field remains squeezed for longer time with larger detunings. The atomic squeezing, however, does not seem to change much with increasing detunings as can be seen in Fig. 12(b). When one- and two-photon resonance conditions are both satisfied, the field squeezing is more remarkable than the atom as is shown in Figs. 12(a) and 13(a). When the detunings are far from resonance conditions as in Figs. 12(c) and 13(c), on the contrary, the atom shows more remarkable squeezing almost immediately after its interaction with the field takes place, while the field squeezing shows up only somewhat later.

#### Acknowledgements

This research was partially supported by the Office of Naval Research, the National Science Foundation under Grant CHE-8620274 and the Air Force Office of Scientific Research (AFSC), United States Air Force, under Contract F49620-86-C-0009. The United States Government is authorized to copy and distribute reprints for governmental purposes notwithstanding any copyright notation hereon.

### References

1. J.H. Eberly, N.B. Narozhny, and J.J. Sanchez-Mondragon, Phys. Rev. Lett. 44, 1323 (1980).
2. X.S. Li and Y.N. Peng, Phys. Rev. A 32, 1501 (1985).
3. H.I. Yoo and J.H. Eberly, Phys. Rep. 118, 239 (1985).
4. X.S. Li, D.L. Lin and C.D. Gong, Phys. Rev. A 36, 5209 (1987).
5. Z. Deng, Opt. Commun. 54, 222 (1986).
6. D. L. Lin, X.S. Li and Y.N. Peng, Phys. Rev. A (in press)
7. P. Meystre and M.S. Zubairy, Phys. Lett. A 89, 390 (1982).
8. P.L. Knight, Phys. Scr. T 12, 51 (1986); K. Wodkiewicz, P.L. Knight, S.J. Buckle and S.M. Barnett, Phys. Rev. A 35, 2567 (1987).
9. R. Loudon and P.L. Knight, J. Mod. Opt. 34, 709 (1987).
10. A.S. Shumovsky, F.L. Kien and E. I. Aliskenderov, Phys. Lett. 124A, 351 (1987).
11. S.Y. Zhu, Z.D. Liu and X.S. Li, Phys. Lett. 128A, 89 (1988).
12. Z. D. Liu, S.Y. Zhu, and X.S. Li, J. Mod. Opt. 35, 833 (1988).
13. S.Y. Zhu, Phys. Lett. A, 130, 101 (1988).
14. L. Davidovich, J.M. Raimond, M. Brune, and S. Haroche, Phys. Rev. A 36, 3771 (1987).
15. G. Rempe and H. Walther, Phys. Rev. Lett. 58, 353 (1987).
16. H. Takahasi, Adv. Commun. Syst. 1, 227 (1965); D.R. Robinson, Commun. Math. Phys. 1, 159 (1965).
17. D. Stoler, Phys. Rev. D 1, 3217 (1970); D 4, 1925 (1971); E.Y.C. Lu, Lett. Nuovo Cim. 2, 1241 (1971); 3, 585 (1972).
18. H. P. Yuen, Phys. Rev. A 13, 2226 (1976).
19. J.N. Hollenhorst, Phys. Rev. D 19, 1669 (1979).
20. C.M. Caves, Phys. Rev. D 23, 1693 (1981).

21. R.E. Slusher, L.W. Hollberg, B. Yurke, J.C. Mertz and J.F. Valley,  
Phys. Rev. Lett. 55, 2409 (1985).
22. L. A. Wu, H.J. Kimble, J.L. Hall and H. Wu, Phys. Rev. Lett. 57,  
2520 (1986).
23. D.F. Walls, Nature 306, 141 (1983).
24. D.F. Walls and P. Zoller, Phys. Rev. Lett. 47, 709 (1981).
25. M. Kozierowski, Phys. Rev. A 34, 3473 (1986).
26. C.K. Hong and L. Mandel, Phys. Rev. A 32, 974 (1985); Phys. Rev. Lett.  
54 323 (1985).
27. H. P. Yuen and J.H. Shapiro, IEEE Trans. Inf. Theory 26, 78 (1980).
28. J. Gea-Banacloche and G. Leuchs, J. Mod. Opt. 34, 793 (1987).
29. C.W. Gardiner, Phys. Rev. Lett. 56, 1917 (1986); G.J. Milburn, Phys.  
Rev. A 34, 4882 (1986); B. Yurke and E.A. Whittaker, Opt. Lett. 12, 236  
(1987).
30. Z.D. Liu, X.S. Li and D.L. Lin, Phys. Rev. A 36, 5220 (1987).
31. S. Stenholm, Phys. Rep. 6, 1 (1973).
32. P. Meystre, E. Geneux, A. Quattropani and A. Faist, Nuovo Cim. 25 B,  
521 (1975).
33. N. B. Narozhny, J.J. Sanchez-Mondragon and J.H. Eberly, Phys. Rev.  
A 23, 236 (1981).

### Figure Captions

1. Energy level configurations of a three-level atom. (a)  $\Xi$ -type and (b)  $\Lambda$ -type.
2. Time evolution of components and correlation function of the atomic dipole moment for the one-mode  $\Xi$ -type case with the initial atomic state  $|b\rangle$ . The parameters are  $\bar{n} = 30$ ,  $\Delta_1 = 5$  and  $\Delta_2 = -5$ .
3. Same as Fig. 2 except  $\Delta_1 = \Delta_2 = 50$ .
4. Squeezing development of  $D_{ab}^I$  (dashed line) and  $D_{ab}^{II}$  (solid line) for  $n = 30$ ,  $\Delta_1 = 5$  and (a)  $\Delta_2 = -10$ , (b)  $\Delta_2 = -5$ , (c)  $\Delta_2 = 0$ , (d)  $\Delta_2 = 5$ , (e)  $\Delta_2 = 20$ .
5. Dependence of maximum squeezing upon the excitation intensity. The solid line represents the minimum  $D_{ab}^{II}$ , and the dashed line represents the time at which the maximum squeezing occurs.
6. Time evolution of components and correlation function of the dipole moment for the two-mode  $\Lambda$ -type case with the initial atomic state  $|a\rangle$ . The parameters are  $\bar{n}_1 = \bar{n}_2 = 10$ ,  $\Delta_1 = 0$  and  $\Delta_2 = 5$ .
7. Same as in Fig. 6 except  $\Delta_1 = 5$ .
8. Time evolution of components and correlation function of the dipole moment for the two-mode  $\Lambda$ -type case with the initial atomic state  $|b\rangle$ . The parameters are  $\bar{n}_1 = \bar{n}_2 = 10$ ,  $\Delta_1 = -10$  and  $\Delta_2 = 5$ .
9. Same as in Fig. 8 except  $\Delta_1 = 0$ .
10. Same as in Fig. 8 except  $\Delta_1 = \Delta_2 = 50$ .

11. Development of squeezing for the two-mode  $\Lambda$ -type case with the initial

atomic state  $|b\rangle$ .  $D_{ab}^I$  (solid line) and  $D_{ab}^{II}$  (dashed line) are plotted

versus time. The parameters are (a)  $\bar{n}_1 = \bar{n}_2 = 10$ ,  $\Delta_1 = 8$ ,  $\Delta_2 = 0$ ,

(b)  $\bar{n}_1 = \bar{n}_2 = 10$ ,  $\Delta_1 = 10$ ,  $\Delta_2 = 0$ , (c)  $\bar{n}_1 = \bar{n}_2 = 10$ ,  $\Delta_1 = 20$ ,  $\Delta_2 = 0$ ,

(d)  $\bar{n}_1 = 6$ ,  $\bar{n}_2 = 10$ ,  $\Delta_1 = 10$ ,  $\Delta_2 = 0$ , (e)  $\bar{n}_1 = 15$ ,  $\bar{n}_2 = 10$ ,  $\Delta_1 = 10$ ,  $\Delta_2 = 0$ ,

(f)  $\bar{n}_1 = \bar{n}_2 = 10$ ,  $\Delta_1 = 10$ ,  $\Delta_2 = 4$ , (g)  $\bar{n}_1 = 10$ ,  $\bar{n}_2 = 15$ ,  $\Delta_1 = 10$ ,  $\Delta_2 = 0$ ,

(h)  $\bar{n}_1 = \bar{n}_2 = 15$ ,  $\Delta_1 = 10$ ,  $\Delta_2 = 0$ .

12. Atomic dipole moment squeezing parameter as a function of time. Solid

line represents  $D^I$  and dashed line represents  $D^{II}$ . The mean photon

number  $\bar{n} = 20$  and the detuning parameters are (a)  $\Delta_1 = \Delta_2 = 0$ ,

(b)  $\Delta_1 = \Delta_2 = 20$ , (c)  $\Delta_1 = 20$ ,  $\Delta_2 = -20$ .

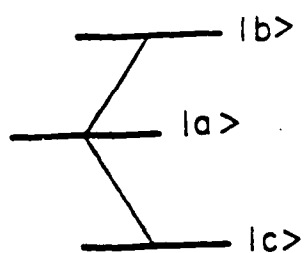
13. The variance of the field one-mode cavity as a function of time.

Solid line represents  $(\Delta d_1)^2$  and dashed line represents  $(\Delta d_2)^2$ . The

mean photon number  $\bar{n} = 20$  and the detuning parameters are

(a)  $\Delta_1 = \Delta_2 = 0$ , (b)  $\Delta_1 = \Delta_2 = 20$ , (c)  $\Delta_1 = 20$ ,  $\Delta_2 = -20$ .

(a)



(b)

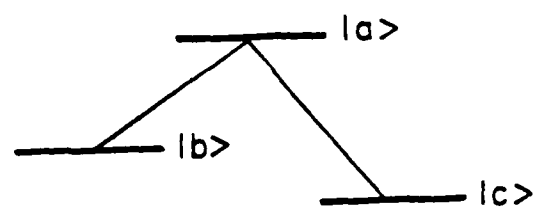


Fig. 1.

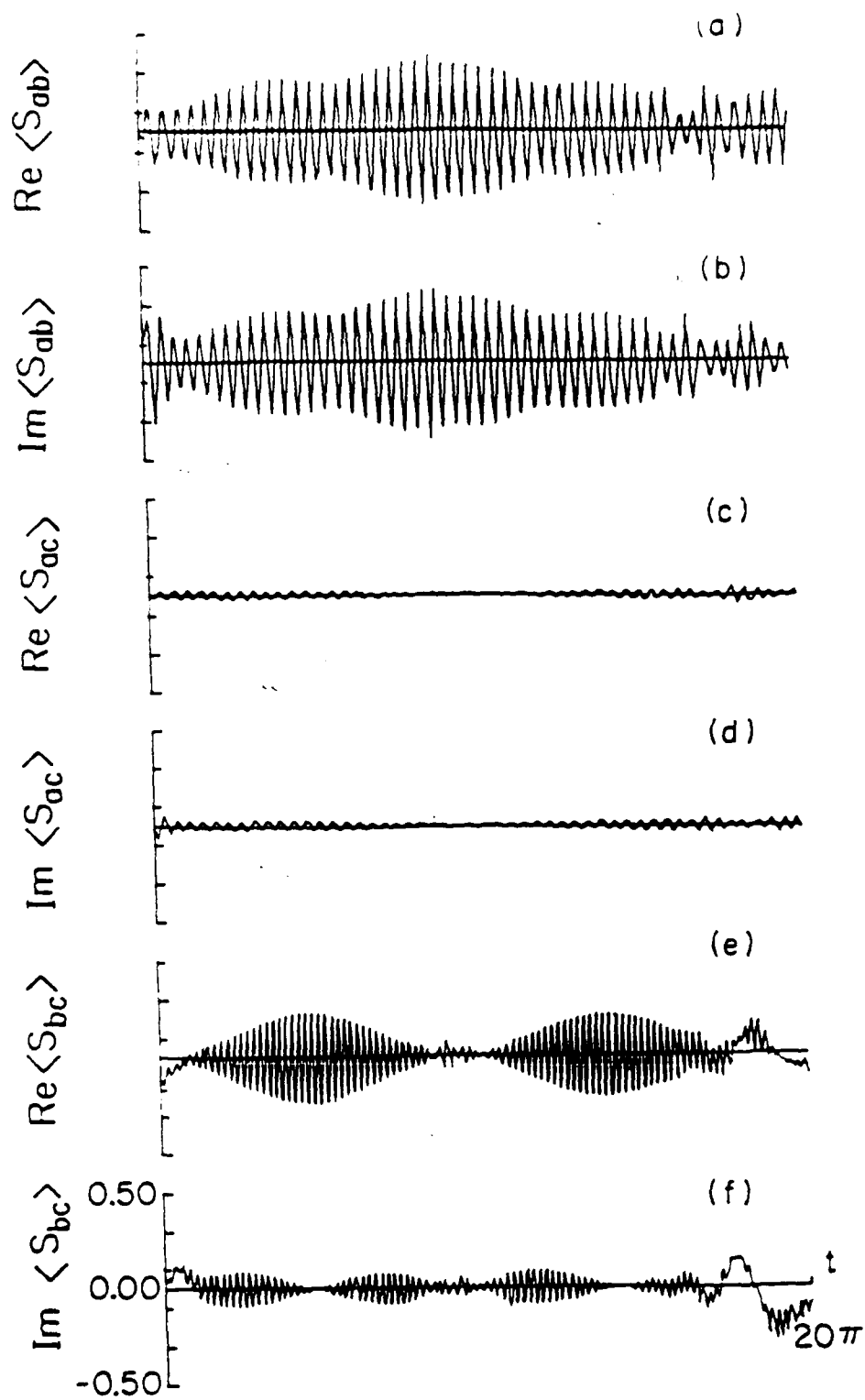


Fig. 2.

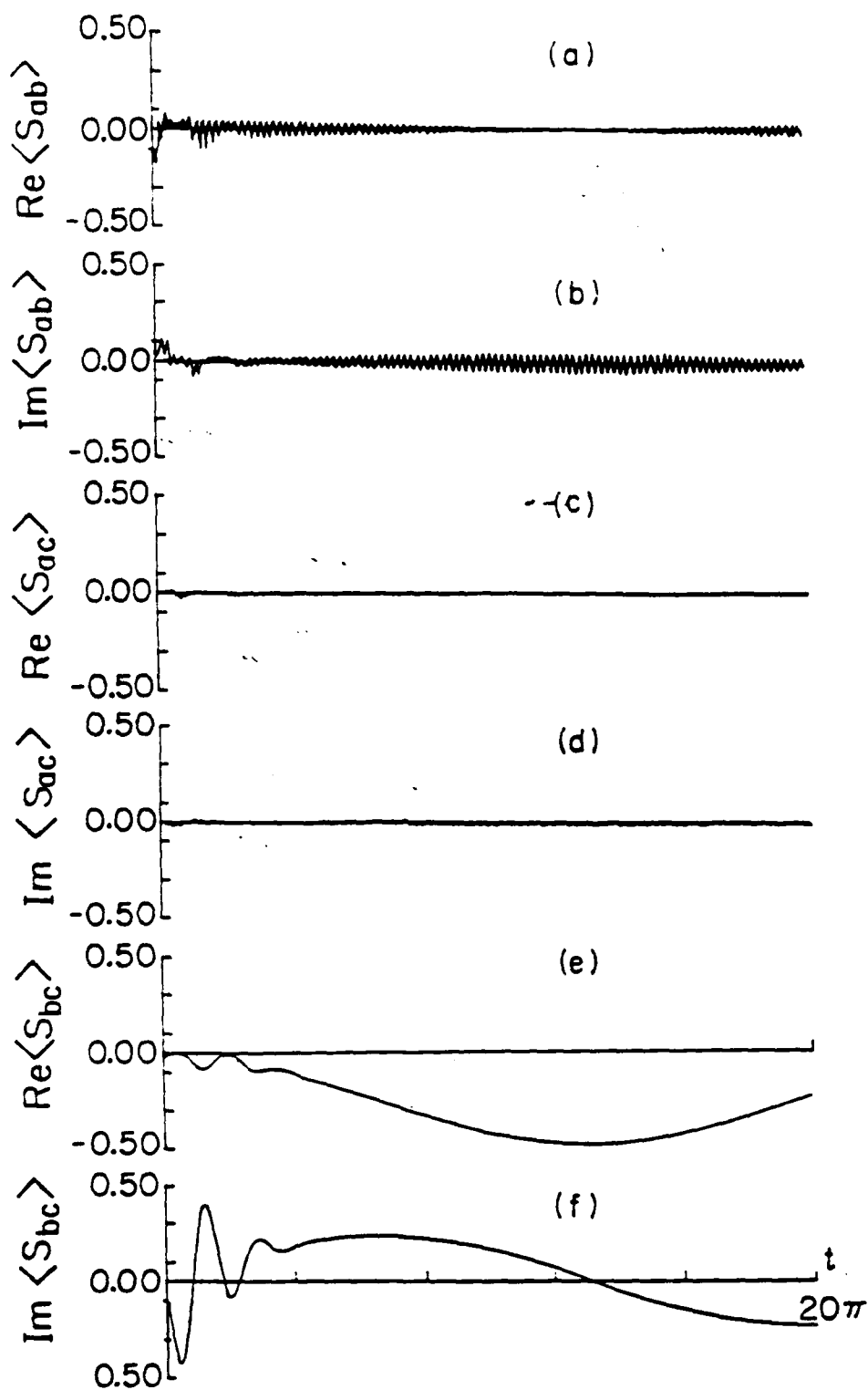


Fig. 3.

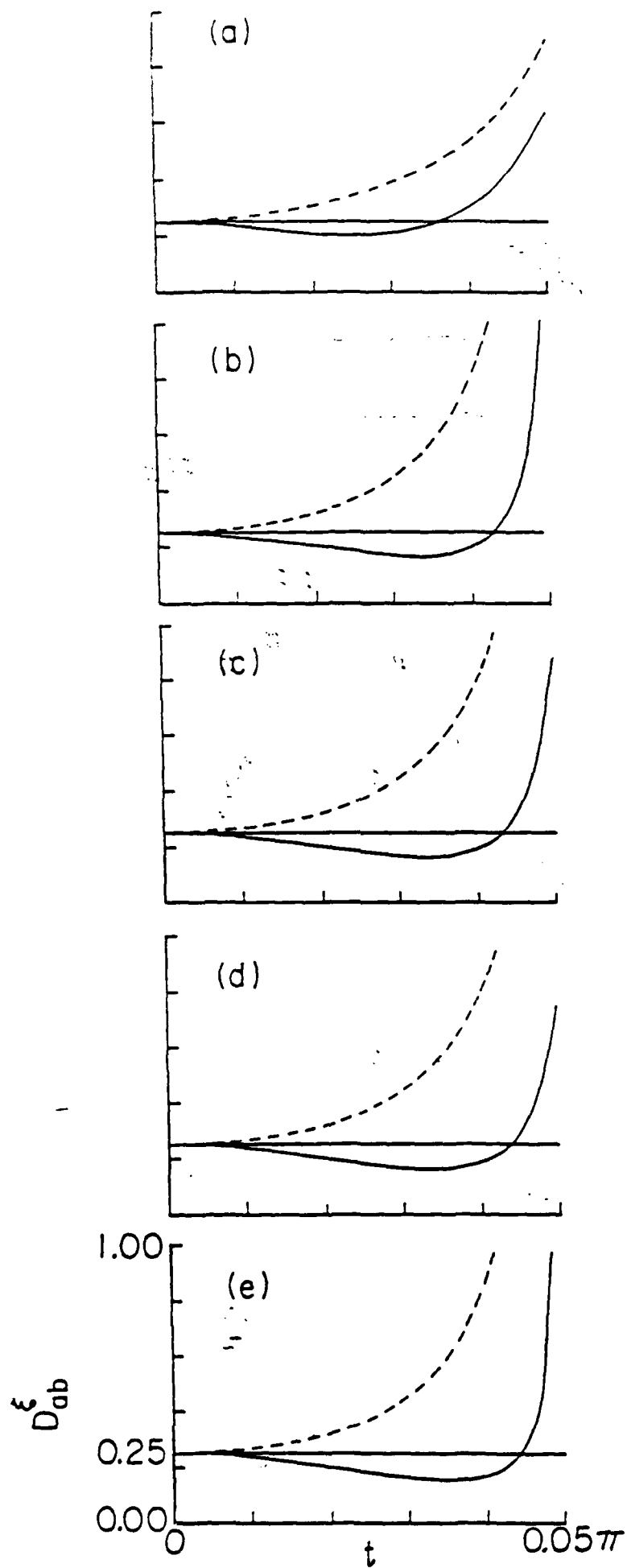


Fig. 4.

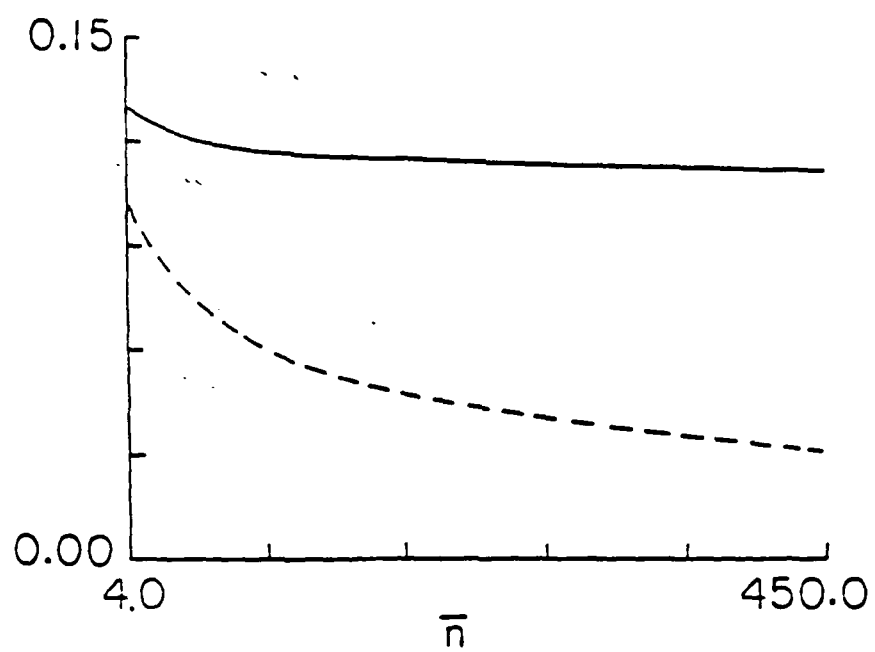


Fig. 5.

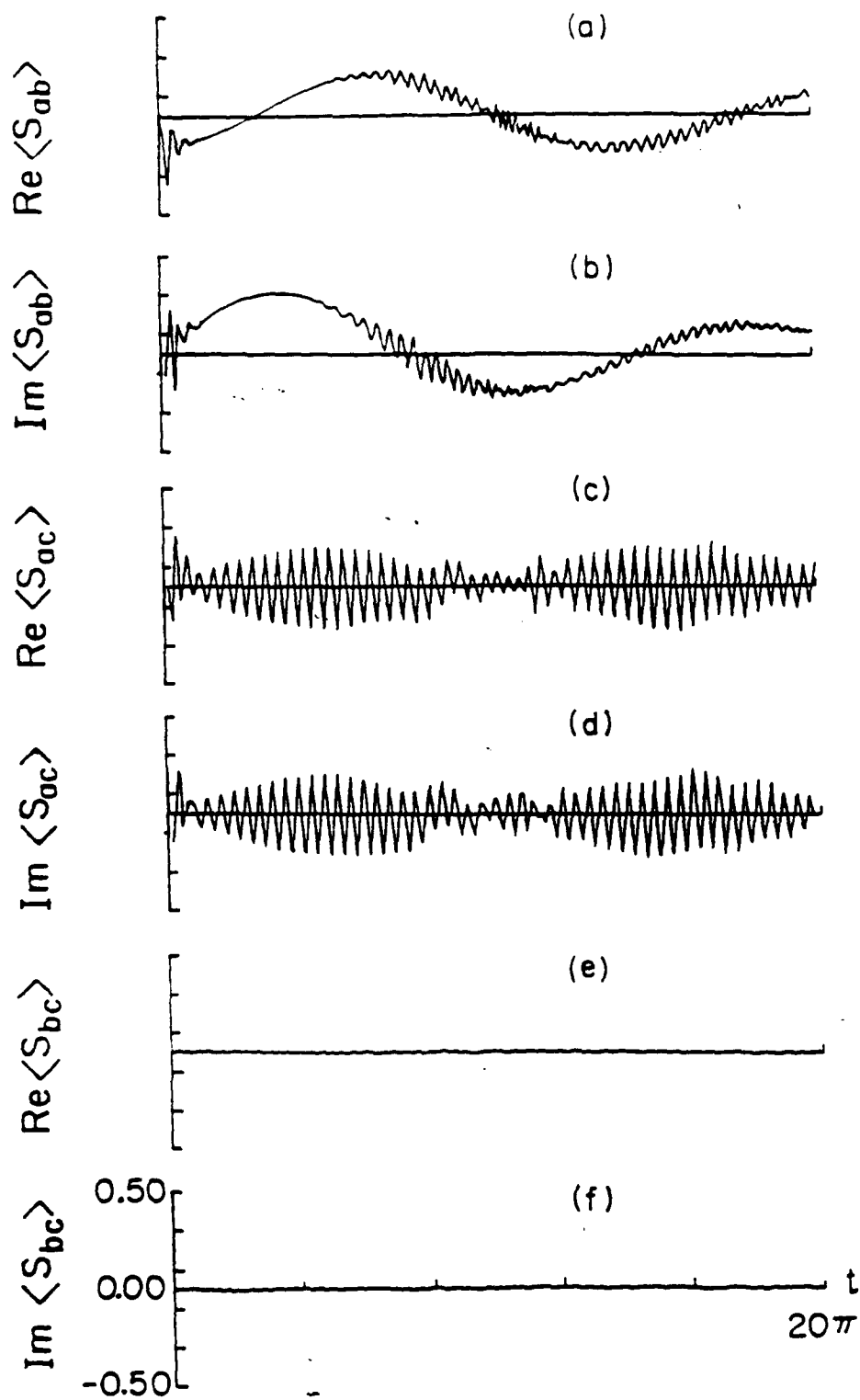


Fig. 6.

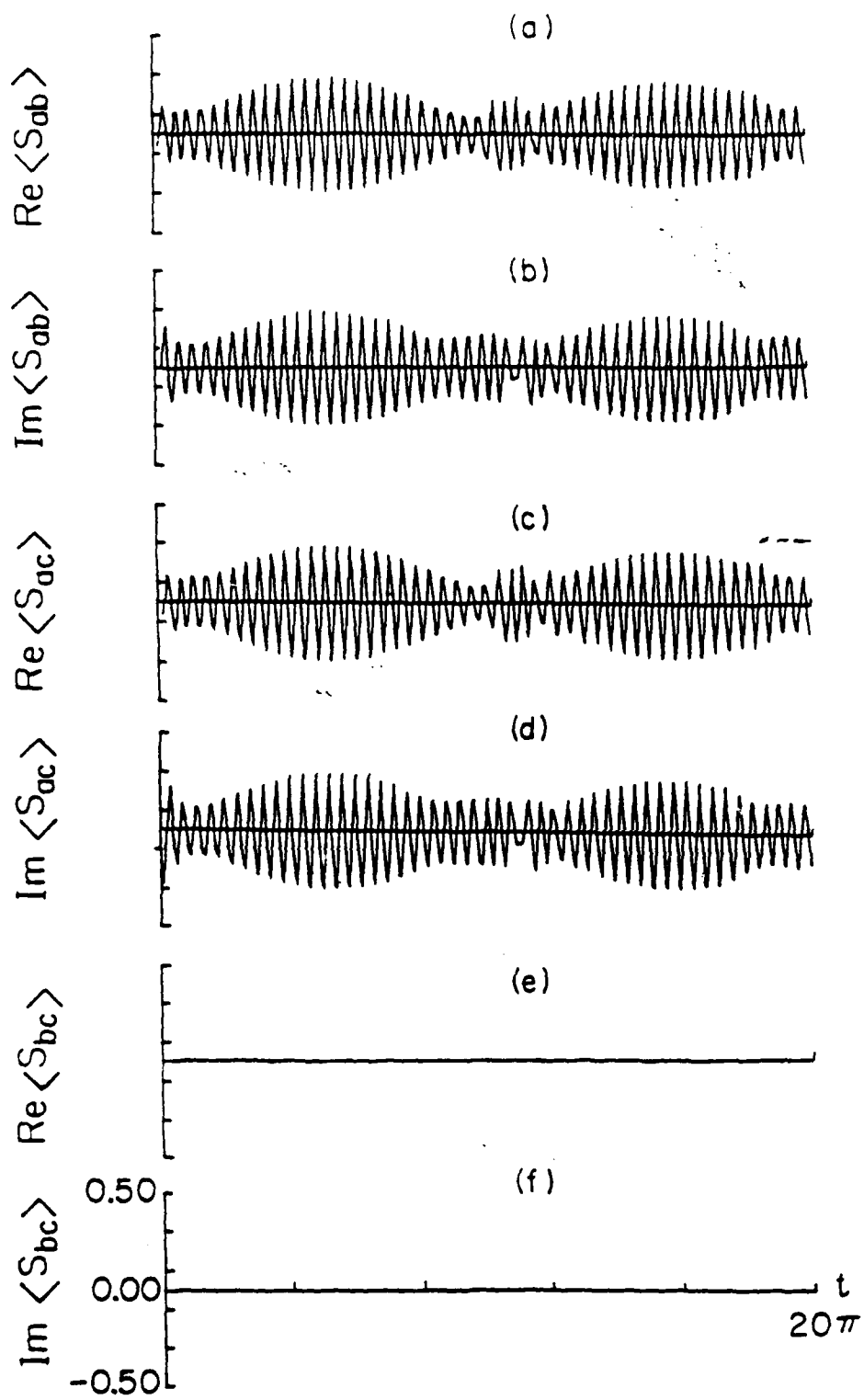


Fig. 7.

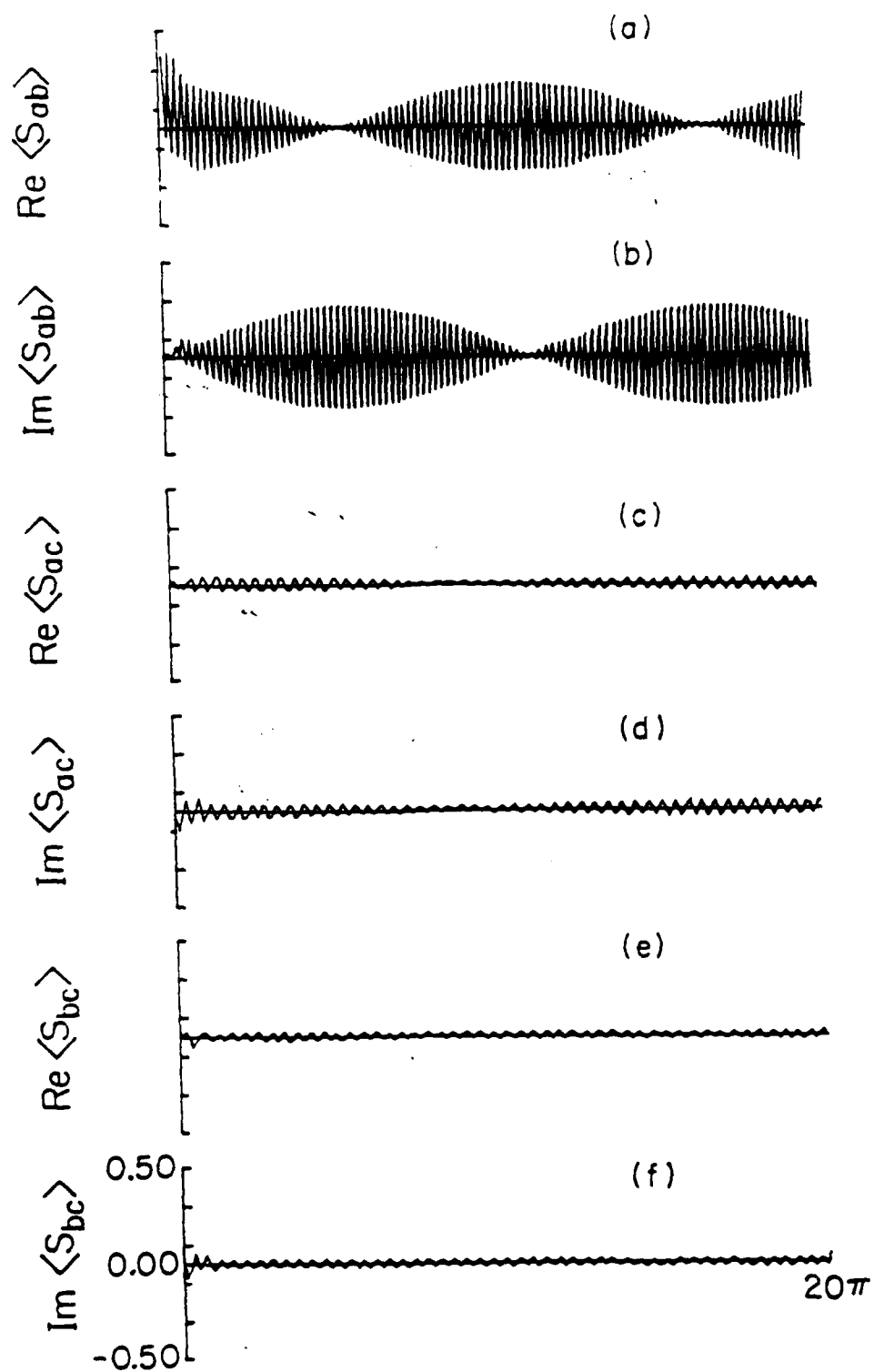


Fig. 8.

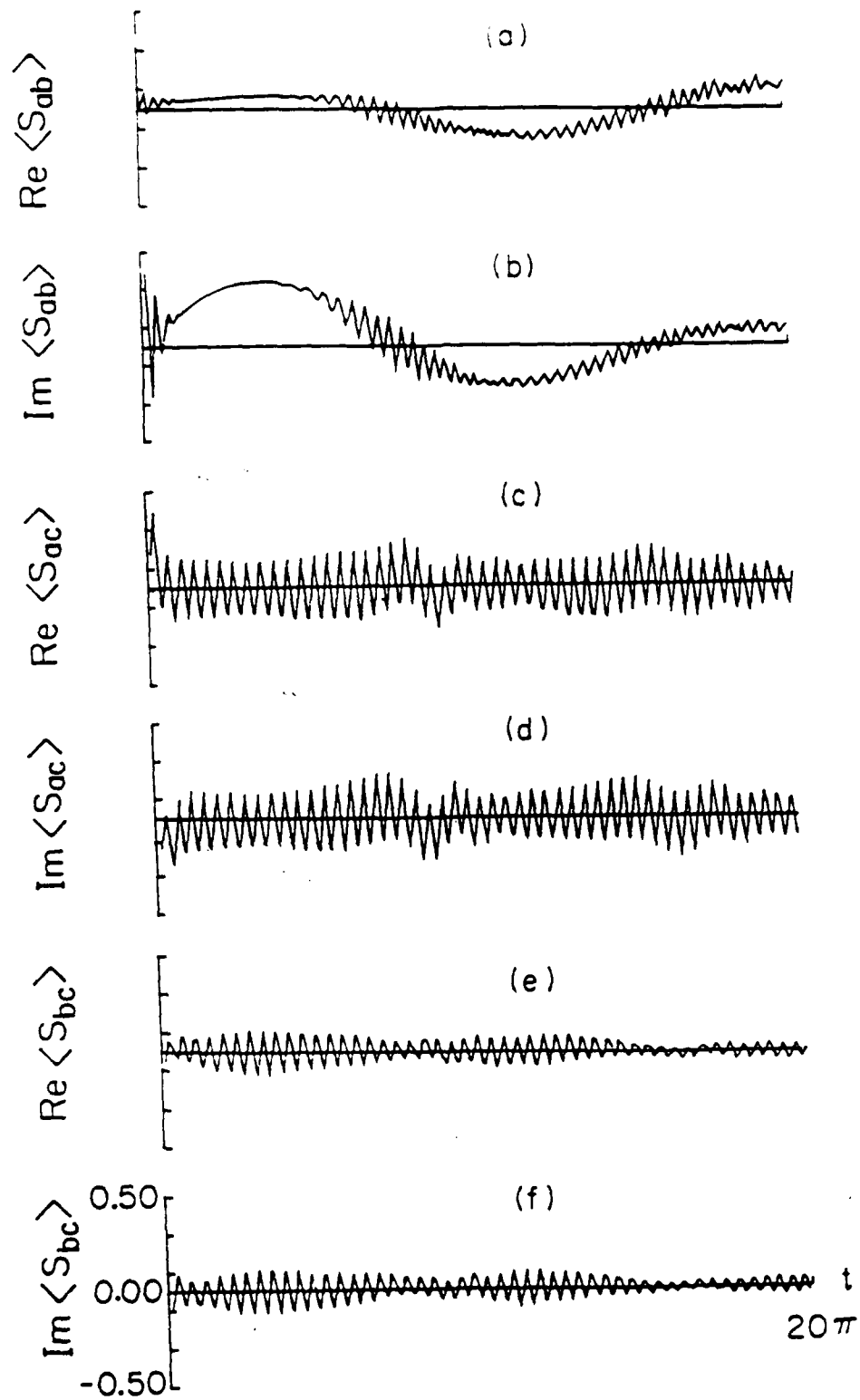


Fig. 9.

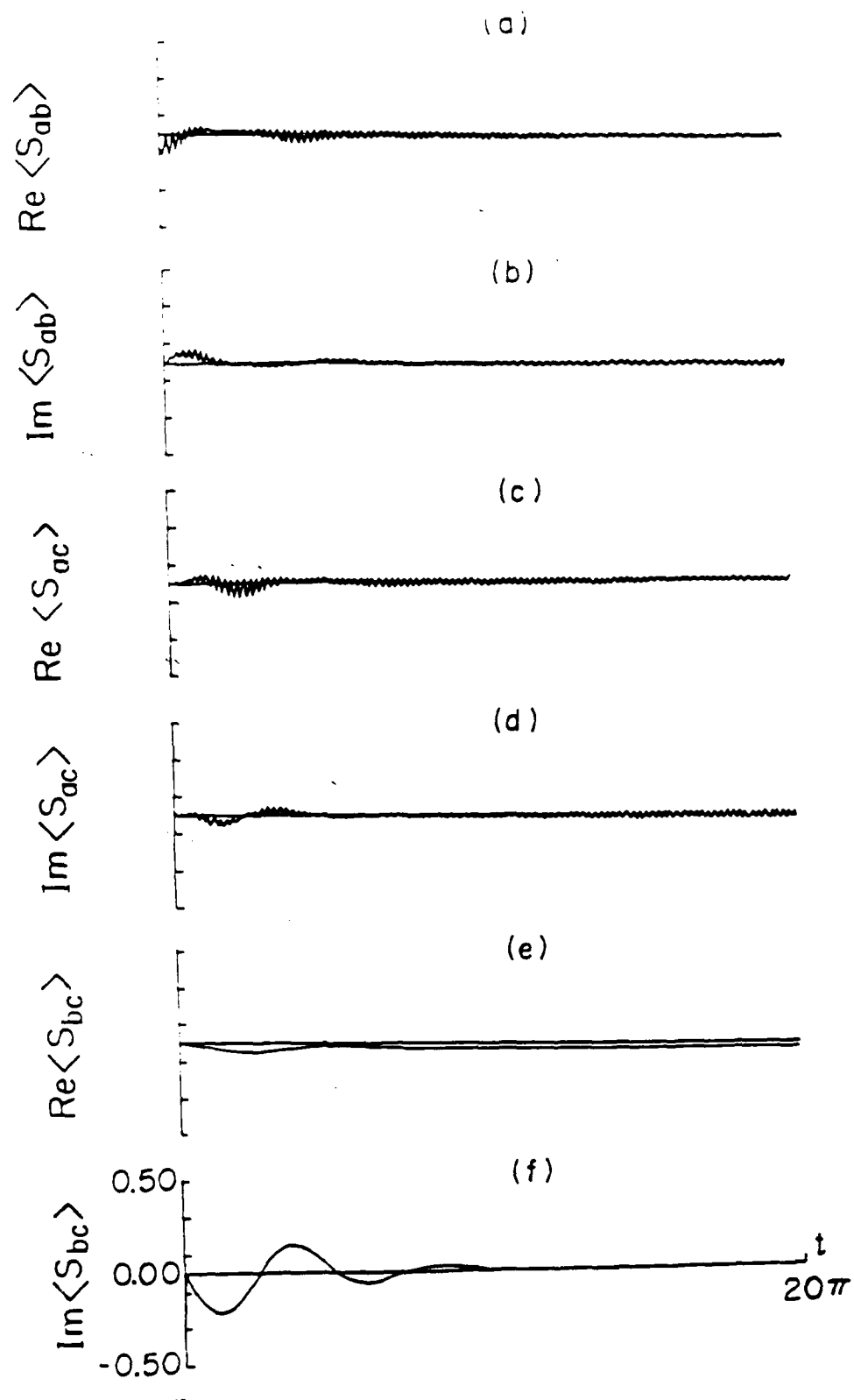


Fig. 10.

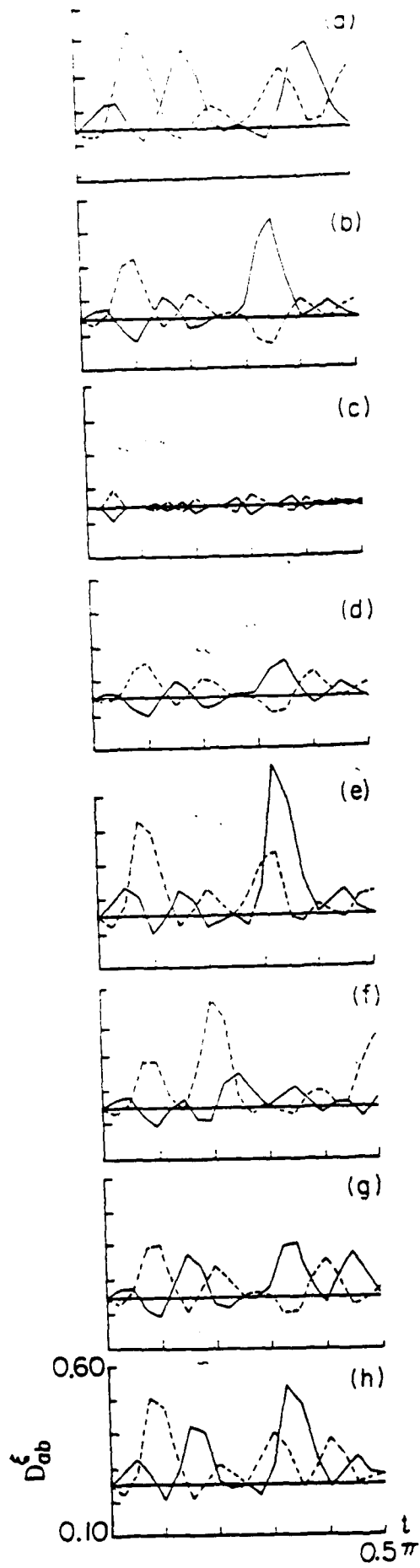
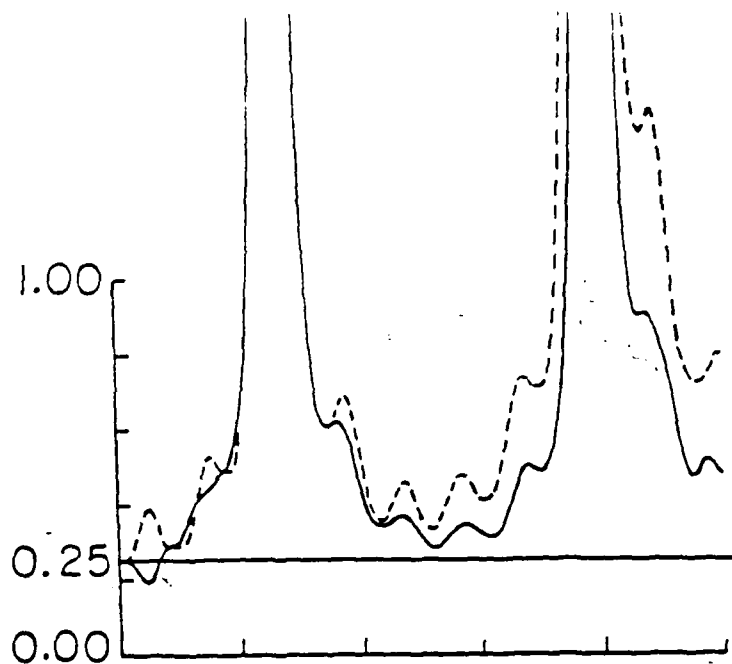
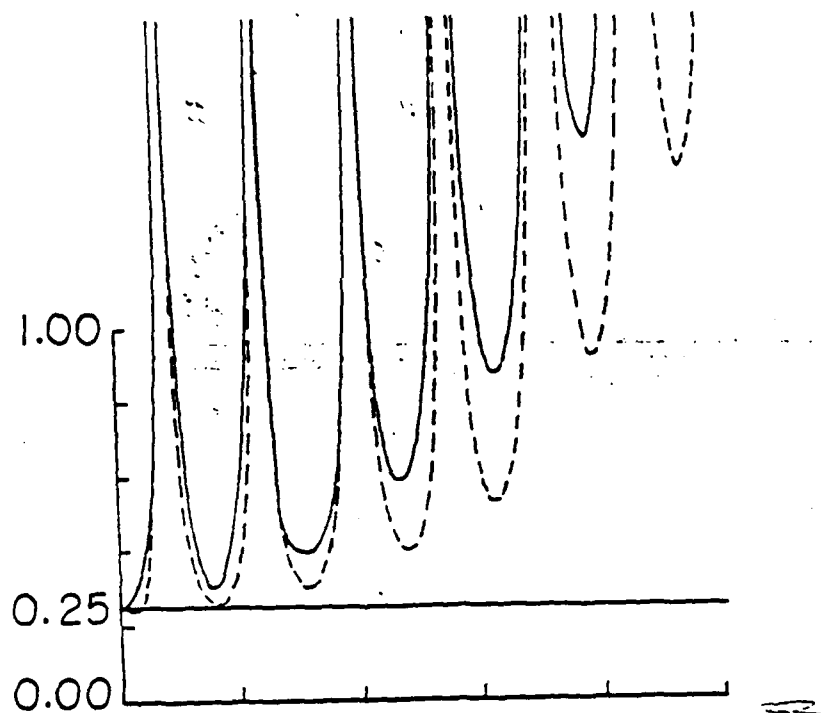


Fig. 11.

(a)



(b)



(c)

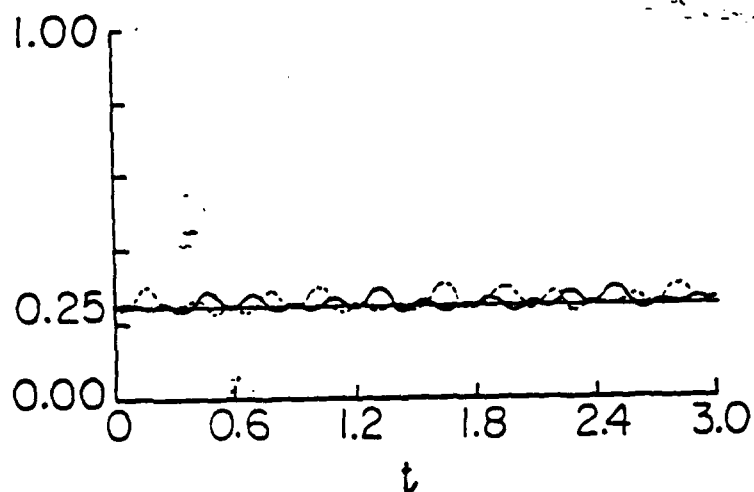


Fig. 12.

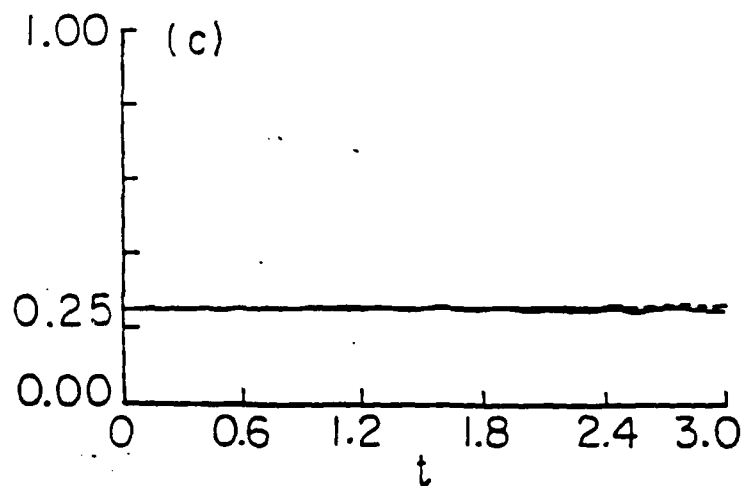
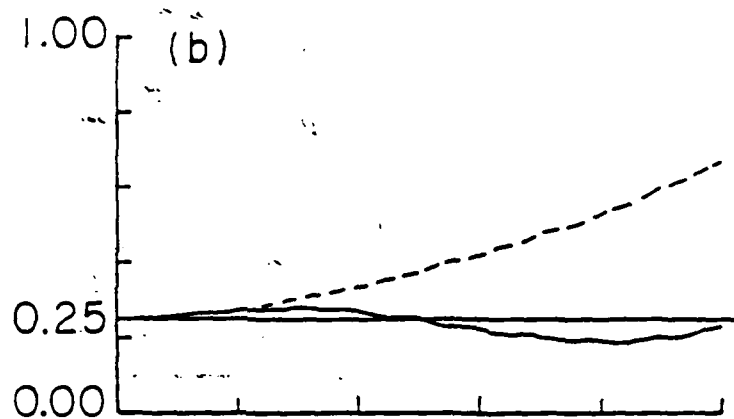
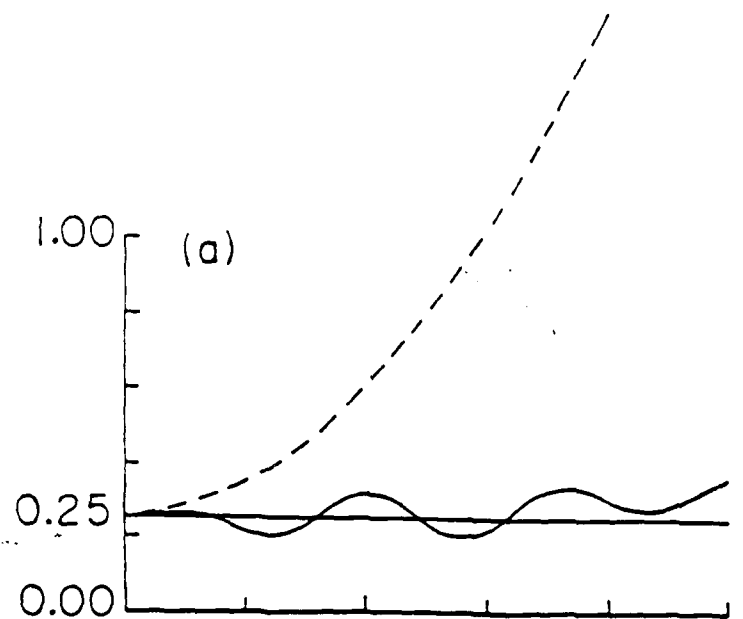


Fig. 13.

TECHNICAL REPORT DISTRIBUTION LIST, GEN

	<u>No. Copies</u>		<u>No. Copies</u>
Office of Naval Research Attn: Code 1113 800 M. Quincy Street Arlington, Virginia 22217-5000	2	Dr. David Young Code 334 NORDA NSTL, Mississippi 39529	1
Dr. Bernard Douda Naval Weapons Support Center Code 50C Crane, Indiana 47522-5050	1	Naval Weapons Center Attn: Dr. Ron Atkins Chemistry Division China Lake, California 93555	1
Naval Civil Engineering Laboratory Attn: Dr. R. W. Drisko, Code L52 Port Hueneme, California 93401	1	Scientific Advisor Commandant of the Marine Corps Code RD-1 Washington, D.C. 20380	1
Defense Technical Information Center Building 5, Cameron Station Alexandria, Virginia 22314	12 high quality	U.S. Army Research Office Attn: CRD-AA-IP P.O. Box 12211 Research Triangle Park, NC 27709	1
DTNSRDC Attn: Dr. H. Singerman Applied Chemistry Division Annapolis, Maryland 21401	1	Mr. John Boyle Materials Branch Naval Ship Engineering Center Philadelphia, Pennsylvania 19112	1
Dr. William Tolles Superintendent Chemistry Division, Code 6100 Naval Research Laboratory Washington, D.C. 20375-5000	1	Naval Ocean Systems Center Attn: Dr. S. Yamamoto Marine Sciences Division San Diego, California 91232	1
		Dr. David L. Nelson Chemistry Division Office of Naval Research 800 North Quincy Street Arlington, Virginia 22217	1

ABSTRACTS DISTRIBUTION LIST, 056/625/629

Dr. J. E. Jensen  
Hughes Research Laboratory  
3011 Malibu Canyon Road  
Malibu, California 90265

Dr. J. H. Weaver  
Department of Chemical Engineering  
and Materials Science  
University of Minnesota  
Minneapolis, Minnesota 55455

Dr. A. Reisman  
Microelectronics Center of North Carolina  
Research Triangle Park, North Carolina  
27709

Dr. M. Grunze  
Laboratory for Surface Science and  
Technology  
University of Maine  
Orono, Maine 04469

Dr. J. Butler  
Naval Research Laboratory  
Code 6115  
Washington D.C. 20375-5000

Dr. L. Interante  
Chemistry Department  
Rensselaer Polytechnic Institute  
Troy, New York 12181

Dr. Irvin Heard  
Chemistry and Physics Department  
Lincoln University  
Lincoln University, Pennsylvania 19352

Dr. K.J. Klaubunde  
Department of Chemistry  
Kansas State University  
Manhattan, Kansas 66506

Dr. C. B. Harris  
Department of Chemistry  
University of California  
Berkeley, California 94720

Dr. F. Kutzler  
Department of Chemistry  
Box 5055  
Tennessee Technological University  
Cookeville, Tennessee 38501

Dr. D. DiLella  
Chemistry Department  
George Washington University  
Washington D.C. 20052

Dr. R. Reeves  
Chemistry Department  
Rensselaer Polytechnic Institute  
Troy, New York 12181

Dr. Steven M. George  
Stanford University  
Department of Chemistry  
Stanford, CA 94305

Dr. Mark Johnson  
Yale University  
Department of Chemistry  
New Haven, CT 06511-8118

Dr. W. Knauer  
Hughes Research Laboratory  
3011 Malibu Canyon Road  
Malibu, California 90265

ABSTRACTS DISTRIBUTION LIST, 056/625/629

Dr. G. A. Somorjai  
Department of Chemistry  
University of California  
Berkeley, California 94720

Dr. J. Murday  
Naval Research Laboratory  
Code 6170  
Washington, D.C. 20375-5000

Dr. J. B. Hudson  
Materials Division  
Rensselaer Polytechnic Institute  
Troy, New York 12181

Dr. Theodore E. Madey  
Surface Chemistry Section  
Department of Commerce  
National Bureau of Standards  
Washington, D.C. 20234

Dr. J. E. Demuth  
IBM Corporation  
Thomas J. Watson Research Center  
P.O. Box 218  
Yorktown Heights, New York 10598

Dr. M. G. Lagally  
Department of Metallurgical  
and Mining Engineering  
University of Wisconsin  
Madison, Wisconsin 53706

Dr. R. P. Van Duyne  
Chemistry Department  
Northwestern University  
Evanston, Illinois 60637

Dr. J. M. White  
Department of Chemistry  
University of Texas  
Austin, Texas 78712

Dr. D. E. Harrison  
Department of Physics  
Naval Postgraduate School  
Monterey, California 93940

Dr. R. L. Park  
Director, Center of Materials  
Research  
University of Maryland  
College Park, Maryland 20742

Dr. W. T. Peria  
Electrical Engineering Department  
University of Minnesota  
Minneapolis, Minnesota 55455

Dr. Keith H. Johnson  
Department of Metallurgy and  
Materials Science  
Massachusetts Institute of Technology  
Cambridge, Massachusetts 02139

Dr. S. Sibener  
Department of Chemistry  
James Franck Institute  
5640 Ellis Avenue  
Chicago, Illinois 60637

Dr. Arnold Green  
Quantum Surface Dynamics Branch  
Code 3817  
Naval Weapons Center  
China Lake, California 93555

Dr. A. Wold  
Department of Chemistry  
Brown University  
Providence, Rhode Island 02912

Dr. S. L. Bernasek  
Department of Chemistry  
Princeton University  
Princeton, New Jersey 08544

Dr. W. Kohn  
Department of Physics  
University of California, San Diego  
La Jolla, California 92037

ABSTRACTS DISTRIBUTION LIST, 056/625/629

Dr. F. Carter  
Code 6170  
Naval Research Laboratory  
Washington, D.C. 20375-5000

Dr. Richard Colton  
Code 6170  
Naval Research Laboratory  
Washington, D.C. 20375-5000

Dr. Dan Pierce  
National Bureau of Standards  
Optical Physics Division  
Washington, D.C. 20234

Dr. R. Stanley Williams  
Department of Chemistry  
University of California  
Los Angeles, California 90024

Dr. R. P. Messmer  
Materials Characterization Lab.  
General Electric Company  
Schenectady, New York 22217

Dr. Robert Gomer  
Department of Chemistry  
James Franck Institute  
5640 Ellis Avenue  
Chicago, Illinois 60637

Dr. Ronald Lee  
R301  
Naval Surface Weapons Center  
White Oak  
Silver Spring, Maryland 20910

Dr. Paul Schoen  
Code 6190  
Naval Research Laboratory  
Washington, D.C. 20375-5000

Dr. John T. Yates  
Department of Chemistry  
University of Pittsburgh  
Pittsburgh, Pennsylvania 15260

Dr. Richard Greene  
Code 5230  
Naval Research Laboratory  
Washington, D.C. 20375-5000

Dr. L. Kesmodel  
Department of Physics  
Indiana University  
Bloomington, Indiana 47403

Dr. K. C. Janda  
University of Pittsburgh  
Chemistry Building  
Pittsburg, PA 15260

Dr. E. A. Irene  
Department of Chemistry  
University of North Carolina  
Chapel Hill, North Carolina 27514

Dr. Adam Heller  
Bell Laboratories  
Murray Hill, New Jersey 07974

Dr. Martin Fleischmann  
Department of Chemistry  
University of Southampton  
Southampton SO9 5NH  
UNITED KINGDOM

Dr. H. Tachikawa  
Chemistry Department  
Jackson State University  
Jackson, Mississippi 39217

Dr. John W. Wilkins  
Cornell University  
Laboratory of Atomic and  
Solid State Physics  
Ithaca, New York 14853

ABSTRACTS DISTRIBUTION LIST, 056/625/629

Dr. R. G. Wallis  
Department of Physics  
University of California  
Irvine, California 92664

Dr. D. Ramaker  
Chemistry Department  
George Washington University  
Washington, D.C. 20052

Dr. J. C. Hemminger  
Chemistry Department  
University of California  
Irvine, California 92717

Dr. T. F. George  
Chemistry Department  
University of Rochester  
Rochester, New York 14627

Dr. G. Rubloff  
IBM  
Thomas J. Watson Research Center  
P.O. Box 218  
Yorktown Heights, New York 10598

Dr. Horia Metiu  
Chemistry Department  
University of California  
Santa Barbara, California 93106

Dr. W. Goddard  
Department of Chemistry and Chemical  
Engineering  
California Institute of Technology  
Pasadena, California 91125

Dr. P. Hansma  
Department of Physics  
University of California  
Santa Barbara, California 93106

Dr. J. Baldeschwieler  
Department of Chemistry and  
Chemical Engineering  
California Institute of Technology  
Pasadena, California 91125

Dr. J. T. Keiser  
Department of Chemistry  
University of Richmond  
Richmond, Virginia 23173

Dr. R. W. Plummer  
Department of Physics  
University of Pennsylvania  
Philadelphia, Pennsylvania 19104

Dr. E. Yeager  
Department of Chemistry  
Case Western Reserve University  
Cleveland, Ohio 41106

Dr. N. Winograd  
Department of Chemistry  
Pennsylvania State University  
University Park, Pennsylvania 16802

Dr. Roald Hoffmann  
Department of Chemistry  
Cornell University  
Ithaca, New York 14853

Dr. A. Steckl  
Department of Electrical and  
Systems Engineering  
Rensselaer Polytechnic Institute  
Troy, New York 12181

Dr. G.H. Morrison  
Department of Chemistry  
Cornell University  
Ithaca, New York 14853